

# Interfacial oxide growth and filling-up behaviour of the micro-gap in silicon fusion bonding processes

B. K. JU, M. H. OH

*Division of Applied Science and Engineering, Korea Institute of Science and Technology, 39-1 Haweolgog-dong, Seongbuk-gu, Seoul 136-791, Korea*

K. H. TCHAH

*Department of Electronic Engineering, Korea University, Anam-dong, Seongbuk-gu, Seoul 136-701, Korea*

In the silicon fusion bonding (SFB) process, the influence of post-annealing atmospheres on the micro-gap existing at the Si-Si bonding interface was investigated with the observation of ultrasonic images, angle lap-stained junctions and cross-section SEM morphologies. Additionally, the bonding strength and the electrical properties of diodes were compared after annealing processes at 1100 °C for 10 s to 10 h in wet O<sub>2</sub>, dry O<sub>2</sub> and N<sub>2</sub> atmospheres. Our results show that a significant saving of annealing time necessary to eliminate the non-contact micro-gap region having a width of  $\leq 0.1 \mu\text{m}$  can be obtained if the hydrogen-bonded wafer pair is pre-stabilized and post-annealed in wet O<sub>2</sub> (95 °C water bubbling) rather than in a dry O<sub>2</sub> or N<sub>2</sub> atmosphere. Based on the above results, we propose that the stabilizing and annealing step in highly oxidizing atmosphere has an important role in the oxide filling-up phenomenon between wafer and wafer gap, in addition to the well-known mechanism of wafer plastic deformation at high temperature followed by solid-state diffusion of Si and O atoms.

## 1. Introduction

The silicon fusion bonding (SFB) process, which has been widely used to fabricate the silicon-on-insulator (SOI) substrates, may also have great potential applications in micromachined Si sensors due to its technical feasibility and economical suitability for batch fabrication [1, 2]. The two important process parameters for the application of the SFB technique to sensor fabrication or SOI fields are the elimination of the so-called gap, the non-contact region at the Si-Si interface, and the precise thickness control of the Si membrane as an "active wafer" on which proper circuitry will be formed afterwards.

The gaps existing at the bonding interface can be divided into three categories [3-5]. Macro-gaps having a width of  $\geq 0.5 \mu\text{m}$  are due to contamination by dust particles from the outside, and bubble-shaped gaps are due to the accumulation of released water molecules at the interface during the medium-temperature (200-600 °C) annealing process. The micro-gaps whose width is less than 0.1  $\mu\text{m}$  are mainly caused by insufficient wafer flatness.

It was reported elsewhere [3, 6, 7] that most of the above-mentioned gaps could be reduced or eliminated through the process of wafer plastic deformation and subsequent solid-state diffusion of Si and O atoms, by a long time (30-120 min) of post-annealing at high temperature ( $\geq 1050 \text{ }^\circ\text{C}$ ) regardless of the annealing

atmosphere. Additionally, the thickness of the Si membrane could be precisely controlled within an error of  $\leq \pm 0.02 \mu\text{m}$  by an electrochemical etch stop method using  $\text{p}^-/\text{p}^{++}$  or n/p electrical junction structure [7, 8]. However, there was out-diffusion and autodoping of impurities in the nearby junction area if the wafer pair had undergone a relatively long time of annealing at high temperature.

In this study, we found that, even for wafer pairs bonded in a class 10 clean-room, there were considerable amounts of gaps at the bonding interface and most of the incomplete bonding states might originate from micro-gaps having a width of  $\leq 0.1 \mu\text{m}$ . Also it was found that the annealing atmosphere plays an important role in the rapid elimination of micro-gaps at the temperature range  $\geq 1050 \text{ }^\circ\text{C}$ . Our experimental results showed that the micro-gaps could be filled up and finally removed as an oxide film grew in interface between wafer and wafer during the annealing procedure in a high oxidizing ambient atmosphere.

## 2. Experimental procedure

The starting materials were 4 in. (102 mm) n- and p-type Si wafers of thickness 525-530  $\mu\text{m}$ , resistivity 4.5-5.5  $\Omega \text{ cm}$ , and crystallographic orientation (100); the mean values of the total indicator reading (TIR)

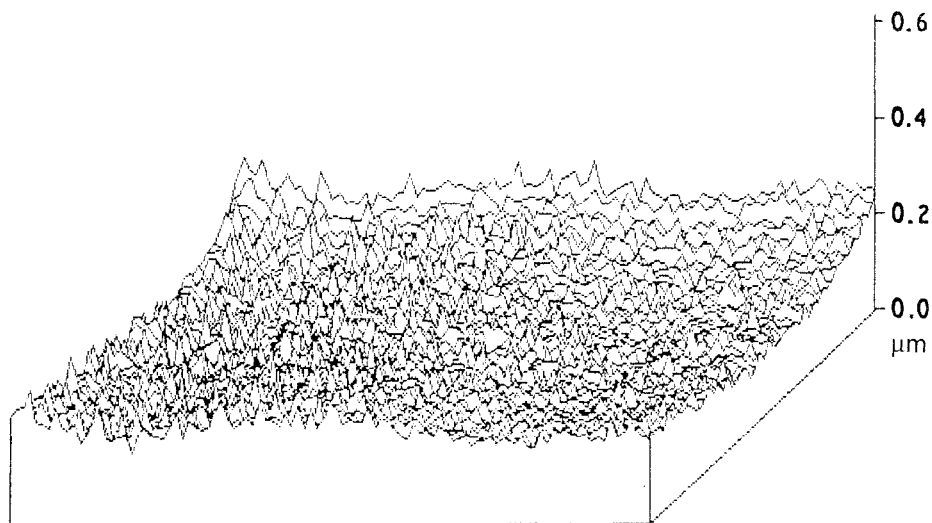


Figure 1 Surface roughness of Si wafer used in this experiment. Dimensions 800  $\mu\text{m}$   $\times$  50  $\mu\text{m}$ .

(a measure of surface flatness) were 1.435–1.553  $\mu\text{m}$ . Fig.1 shows the surface roughness of the wafer used, measured by a surface profiler (SAS Tech Co., Nano surf 488). Prior to bonding, the wafers were cleaned according to the standard RCA method [9] and dipped into an  $\text{H}_2\text{O}:\text{H}_2\text{O}_2:\text{NH}_4\text{OH}$  (6:1:4) solution at 60  $^\circ\text{C}$  for 2 min in order to form a hydrophilic layer on the surface.

After the chemical treatment, the wafers were rinsed in water and dried in a spin dryer. Pre-treated wafers making a p- and n-type pair were brought to a quartz carrier as shown in Fig. 2 and stabilized for 30 s at room temperature while they were separated by a quartz spacer. The stabilizing atmosphere was either wet  $\text{O}_2$  (95  $^\circ\text{C}$  water bubbling), dry  $\text{O}_2$  or  $\text{N}_2$ .

The spacer was then pulled out and hydrogen bonding between the two wafers occurred in 5–10 s after contact. Immediately afterwards, the weakly bonded wafer pair was post-annealed at 1100  $^\circ\text{C}$  for one of the following times: 10 s, 1, 2, 10, 30 min, 1, or 10 h, in order to induce a higher bonding reaction at the interface region. Annealing was carried out in the same atmosphere as that used in the stabilizing step and the temperature was fixed to 1100  $\pm$  2  $^\circ\text{C}$ , chosen with regard to the decomposition of coalescent water clusters, Si elastic–plastic deformation, solid-state diffusion of Si atoms, higher surface oxidation rate and oxide viscous flow at the interface [3–5, 7, 10]. Also, a quartz mass with 400 g weight was put on the upper wafer for the wafer pair to be in intimate contact at the initial annealing stage. All of the above processes were done in class 10 clean-room conditions.

### 3. Results and discussion

Fig. 3a and b show the gap images observed at the bonding interface for wafer pairs stabilized at room temperature for 30 s in wet  $\text{O}_2$  and additionally post-annealed at 1100  $^\circ\text{C}$  for 10 min in the atmosphere, respectively. The images were obtained using an ultrasonic microscope (Testech LS-240 scanning and recording system), which had a higher resolution limit than that of an infrared thermograph [11].

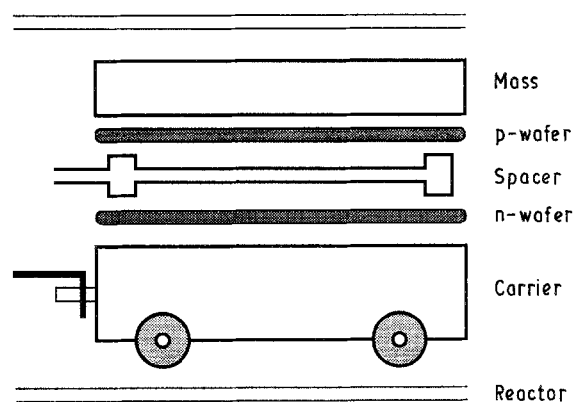


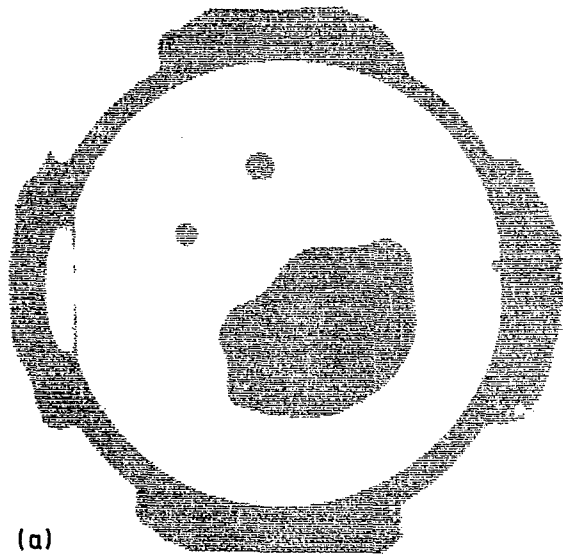
Figure 2 Carrier apparatus for wafer–wafer bonding.

In Fig. 3b, region A represents the region where some gaps had been initially observed just after hydrogen bonding and which disappeared in the annealing process. Region B represents the region in which no gaps were found at the early stage of hydrogen bonding. The region in which the gaps persisted even after the annealing step is expressed as region C, and the boundary of region A and region C is marked as region A–C.

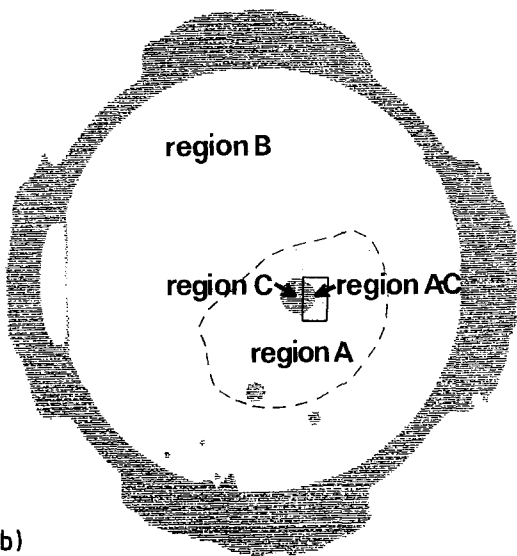
As shown in Fig. 3, the gap area, which occupied initially about 20% of the full wafer, was reduced to about 2% by the 1100  $^\circ\text{C}$  annealing procedure. The change of gap area as a function of annealing time is presented in Fig. 4 for the three types of atmosphere. The vertical axis represents the normalized gap areas on a scale of 1 to 0, where 1 is for an occupancy of about 15–20% and 0 for less than 2%.

It is found in Fig. 4 that, in the case of wafer pairs stabilized and annealed in a wet  $\text{O}_2$  atmosphere, the time required to reduce the gap by 1–2% is only 2 min, while the time in other atmospheres is about 1 h.

Several researchers [3, 5, 6] have reported that the bonding reaction at the junction in a high-temperature annealing step occurred according to the following sequence: surface oxidation in gap  $\rightarrow$  pumping action by partial vacuum in gap  $\rightarrow$  elastic–plastic



(a)



(b)

Figure 3 Gap images of bonded wafer pairs:(a) after stabilizing at room temperature for 30 s and (b) annealing at 1100°C for 10 min in a wet O<sub>2</sub> atmosphere.

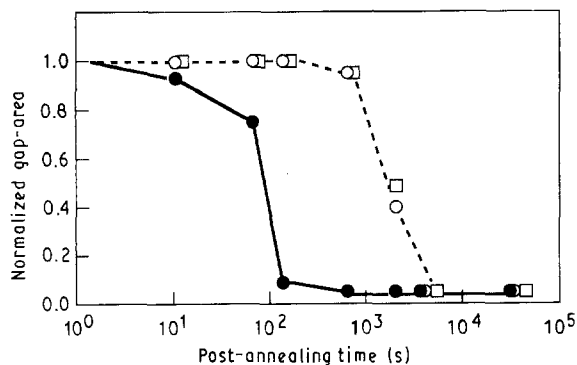
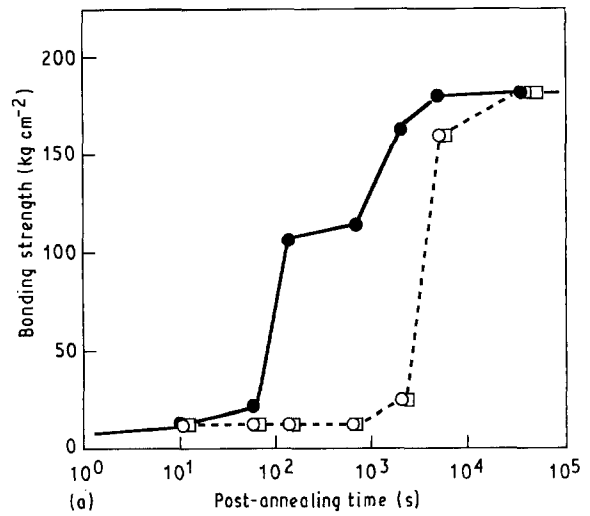
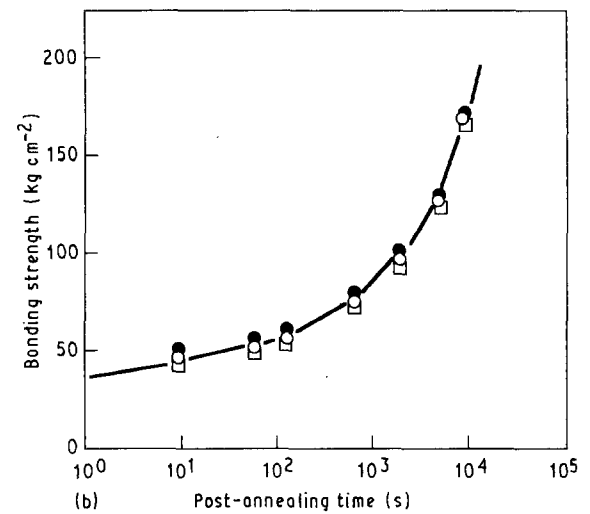


Figure 4 Normalized gap-area versus annealing time for three types of atmosphere: (●) wet O<sub>2</sub>, (○) dry O<sub>2</sub>, (□) N<sub>2</sub>.

deformation of wafers → solid-state diffusion of Si and O atoms into bulk [3, 5, 6]. It was also reported [10] that the bonding strength was improved as the wafer thickness was decreased due to the increase of flexibil-



(a)



(b)

Figure 5 Bonding strength versus annealing time for three types of atmosphere in the case of (a) region A and (b) region B: (●) wet O<sub>2</sub>, (○) dry O<sub>2</sub>, (□) N<sub>2</sub>.

ity. As the bonding strength became higher, the oxidants could not arrive at the bonding interface, and therefore the reduction or elimination of gaps would be more strongly dependent on wafer deformation than the filling-up behaviour by interfacial oxide growth.

However, considering that water vapour is about 600 times more soluble in oxide when compared with dry O<sub>2</sub> and that the water-related species containing hydroxyl ions accelerate the early hydrogen bonding reaction [10, 11], we can suppose that in the case of annealing in a wet O<sub>2</sub> atmosphere oxide growth behaviour on the non-contact wafer surface plays an important role in the rapid elimination of gaps. The vapour oxidants are absorbed during the stabilizing step and also supplied through micro-channels at the junction in the early stage of the annealing step.

In order to see in detail what was the difference of bonding mechanisms at an early stage of annealing between wet O<sub>2</sub> and other atmospheres, we measured the bonding strength using a tensile strength meter (Instron model 4301). Fig. 5a and b show the average

values of bonding strength of the samples extracted from region A and region B, respectively, in which the word "region" has the same meaning as in the case of Fig. 3b. Fig. 5a shows that the bonding strength reaches about  $110 \text{ kg cm}^{-2}$  in 2 min and increases again after 10 min until becoming saturated at  $180 \text{ kg cm}^{-2}$  in 1 h for the wet  $\text{O}_2$  case.

It is very interesting to discuss why the change of bonding strength with time is divided into three zones in a wet  $\text{O}_2$  annealing atmosphere. We suppose that the gap width becomes narrower with elapse of annealing time by wafer deformation, and also that interfacial oxide growth occurs on each Si surface within a gap. In 2 min the oxide layers on both sides are almost in contact with each other, filling up the gaps, but not sufficient to form complete material continuity between the two oxide layers. Grain boundaries existing near the interfaces are removed due to oxide viscous flow as well as the solid-state diffusion of Si and O atoms occurring through further annealing. Eventually, the bonding strength becomes more than  $180 \text{ kg cm}^{-2}$  in 1 h.

In the case of annealing in a dry  $\text{O}_2$  or  $\text{N}_2$  atmosphere, the bonding strength is saturated at a similar value to the wet  $\text{O}_2$  case without any transient phase and, therefore, it can be supposed that the contribution of growing interfacial oxide to gap elimination at the early annealing stage is negligible.

On the other hand, as shown in Fig. 5b, if complete hydrogen bonding without a micro-gap is realized before annealing, the bonding strength increases exponentially with annealing time independently of the annealing atmosphere. This result is in good agreement with those reported by Maszara *et al.* [10] and Stengl *et al.* [11].

In order to examine what happened at the bonding interface during the annealing process, we employed an angle lap-stain method for the junction. Two  $10 \text{ mm} \times 10 \text{ mm}$  samples were selected from region A and region B in the sample shown in Fig. 3b, and the n-type substrates of the n-p wafer pairs obtained were thinned to about  $10 \mu\text{m}$  using a mechanical lapping tool. The sample having a thinned n-type layer was angle-lapped with a bevel angle of  $34'$  and the n-type area stained by dipping it into a solution of  $\text{CuSO}_4 \cdot 5\text{H}_2\text{O}$  (0.8 g) + 49% HF (1 ml) +  $\text{H}_2\text{O}$  (100 ml) s under intense light.

Fig. 6a and b show the specimen structure and the cross-section of a wafer pair having a thin n-type layer before angle lapping, respectively. Also, Fig. 6c and d show the angle lap-stained shapes obtained in region A and region B, respectively.

In the case of region A, it is discovered that an oxide film about 20–30 nm thick fills up the interfacial gap, but only a bonding seam can be observed in region B. In both cases, the annealing time was 10 min. Although the bonding strength in region A could not be saturated by 10 min wet  $\text{O}_2$  annealing, the value of  $110 \text{ kg cm}^{-2}$  is higher than that of region B (about  $70 \text{ kg cm}^{-2}$ ) for the same annealing time. The gap can almost be eliminated, as shown in Fig. 4 for the wet  $\text{O}_2$  annealing process. This is a very interesting phenomenon when we consider that the maximum applicable

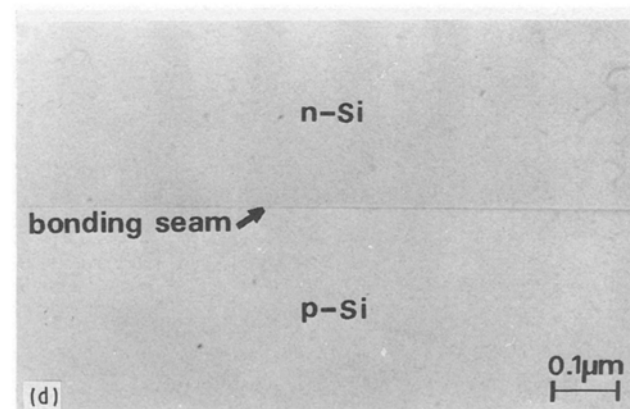
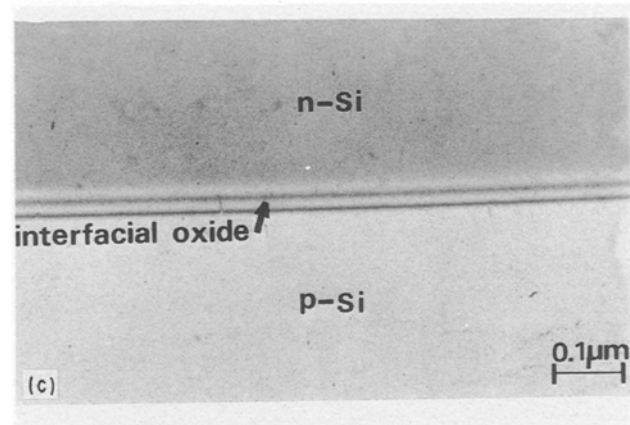
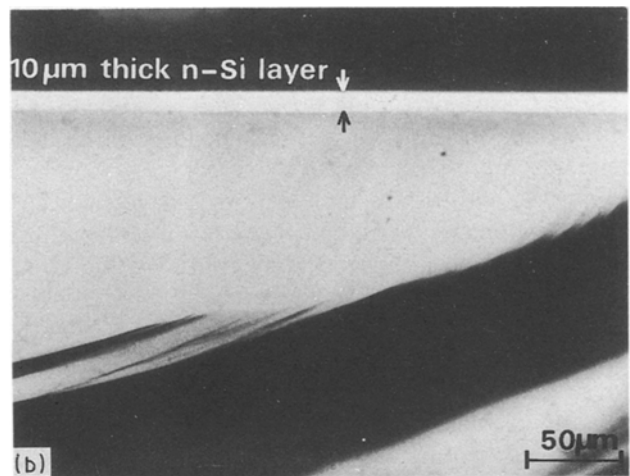
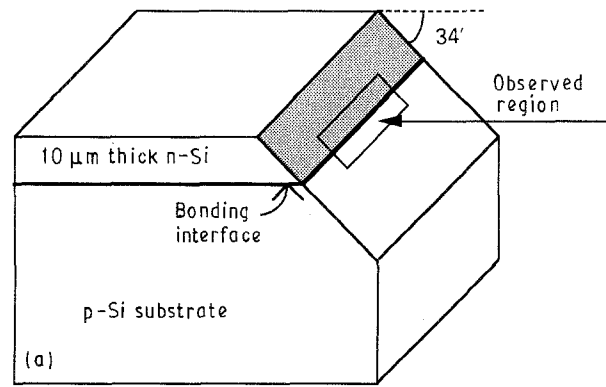


Figure 6 (a) Specimen structure for observation of bonding interface; (b) cross section of bonded wafer pair having a thinned n-type Si layer; (c) angle lap-stained shape for the case of region A in Fig. 3; (d) angle lap-stained shape for the case of region B in Fig. 3.

pressure is  $1\text{--}15\text{ kg cm}^{-2}$  in an Si pressure sensor having a  $10\text{--}30\text{ }\mu\text{m}$  thick membrane [12]; the bonding strength obtained by post annealing at  $1100\text{ }^\circ\text{C}$  for 10 min in wet  $\text{O}_2$  seems to be sufficient for this application.

Fig. 7a shows a cross-section of region A–C in Fig. 3b. We can see that the micro-gap is being filled up when the interfacial oxide grows, as shown on the right-hand side of the dotted line. Also, we can clearly detect the existence of a micro-gap having a width of  $20\text{--}30\text{ nm}$  in Fig. 7b, which is an SEM photograph of the sample after removing the interfacial oxide by dipping it into buffered HF solution for 3 min.

Fig. 8a shows the ultrasonic image of a wafer pair stabilized for 30 s followed by annealing at  $1100\text{ }^\circ\text{C}$  for 10 h in  $\text{N}_2$ . We can see an  $0.8\text{ }\mu\text{m}$  dust particle in region C as shown in Fig. 8b, and this type of gap can be eliminated only by hydrogen bonding in cleaner circumstances.

Fig. 9a and b show the ultrasonic images of wafer pairs obtained after stabilizing at room temperature for 30 s and then post annealing at  $1100\text{ }^\circ\text{C}$  for 3 h in dry  $\text{O}_2$ , respectively. The meaning of region A is the same as in the case of Fig. 3. We made a bonded p-wafer/n-wafer diode, as shown in Fig. 10a, using a selected part of region A. We also carried out additional annealing for 2 h 50 min at  $1100\text{ }^\circ\text{C}$  in a wet  $\text{O}_2$  atmosphere for the sample shown in Fig. 3b and made another diode using part of region A.

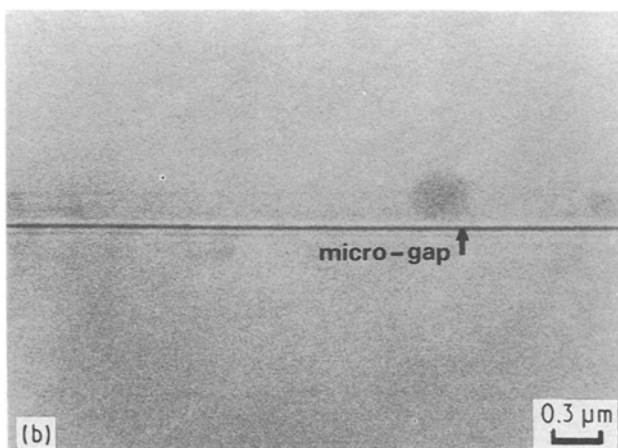
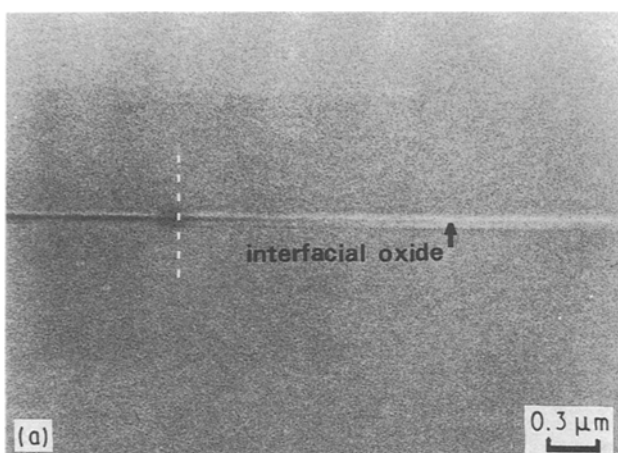


Figure 7 Cross-sectional SEM photographs (a) before and (b) after dipping in buffered HF for the case of region A–C in Fig. 3.

The size of the diode was  $2\text{ mm} \times 2\text{ mm}$  and an Al electrode of  $1.8\text{ mm}$  diameter was evaporated on the p-type side. For ohmic contact, an  $\text{n}^+$  layer was formed on the n-type side by phosphorus diffusion followed by Al evaporation and an Si–Al alloying step.

Fig. 10b and c show the forward  $I\text{--}V$  curves of diodes annealed in wet  $\text{O}_2$  and dry  $\text{O}_2$  atmospheres, respectively. In Fig. 10b, we can see that the dielectric breakdown occurs at  $37\text{--}40\text{ V}$ . The breakdown phenomenon may imply the existence of a  $20\text{--}30\text{ nm}$  thick interfacial oxide, if we suppose that the breakdown field of a thermally grown  $\text{SiO}_2$  film reaches  $15\text{--}13\text{ MV cm}^{-1}$  in the above thickness range [13]. In the case of Fig. 10c, the forward  $I\text{--}V$  curve is well fitted by the normal diode  $I\text{--}V$  equation,  $I = A \exp(qV/nkT)$  where the  $n$  value is about 1.6. This value suggests that the current flows by both recombination and diffusion processes [14]. A reverse leakage current could not be detected even when a reverse bias of  $1000\text{ V}$  was applied.

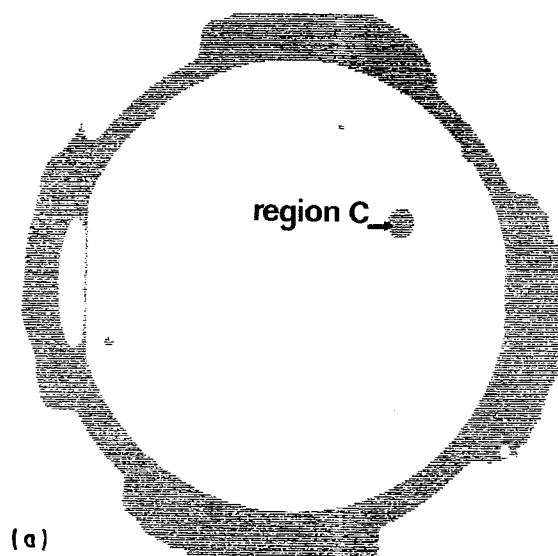
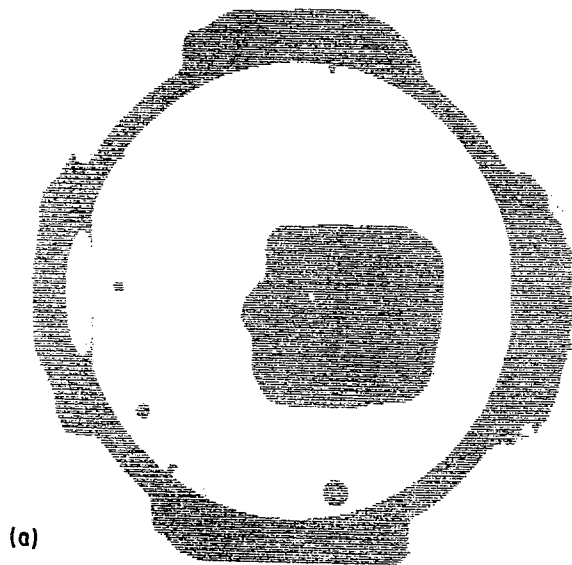
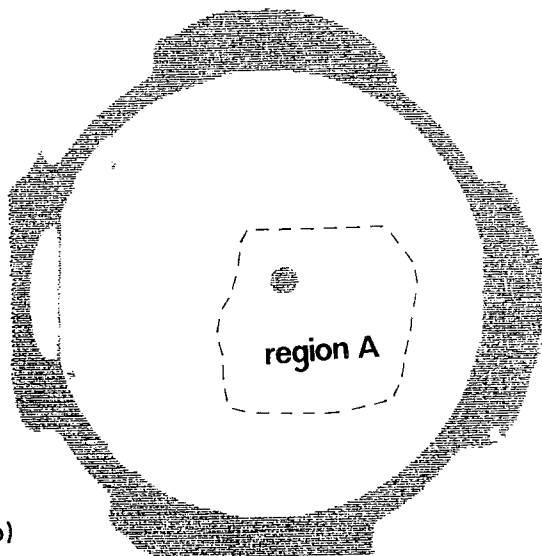


Figure 8 (a) Gap image and (b) cross-section of region C for bonded wafer pair after stabilizing at room temperature for 30 s followed by annealing at  $1100\text{ }^\circ\text{C}$  for 10 h in  $\text{N}_2$ .



(a)



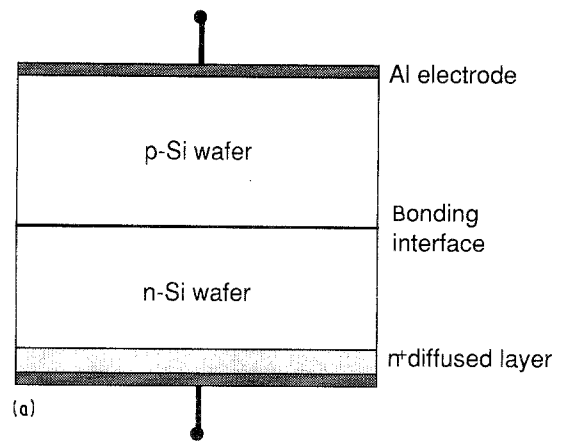
(b)

Figure 9 Gap images of bonded wafer pairs (a) after stabilizing at room temperature for 30 s and (b) annealing at 1100 °C for 3 h in dry O<sub>2</sub>.

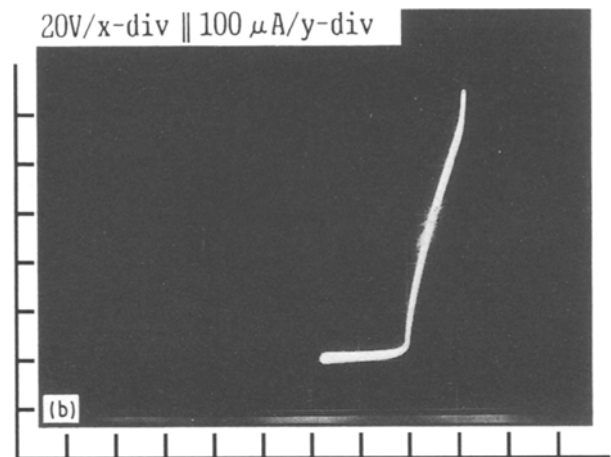
#### 4. Conclusions

We found that interfacial oxide film growth played an important role in the rapid elimination of gaps, when the hydrogen-bonded wafer pair was stabilized and annealed in a strongly oxidant ambient atmosphere. In the case of the wafer pair stabilized at room temperature for 30 s in a wet O<sub>2</sub> atmosphere, almost all of the micro-gaps were removed and the bonding strength reached about 70–110 kg cm<sup>-2</sup> by a post-annealing process at 1100 °C for 2–10 min in the same atmosphere. At that time, the thickness of the interfacial oxide film was measured to be about 20–30 nm and the bonding strength could be increased to about 180 kg cm<sup>-2</sup> by further annealing.

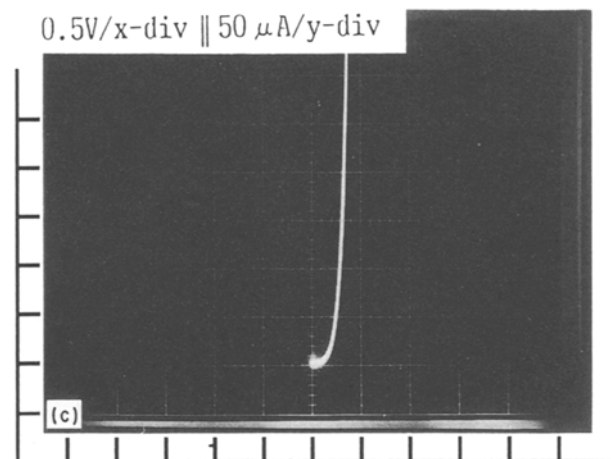
It is supposed that the oxide filling-up phenomenon of the micro-gap can save a long annealing time at high temperature, and so offer improved technical feasibility in subsequent processes.



(a)



(b)



(c)

Figure 10 (a) Diode structure made by wafer bonding and forward *I*-*V* curves for (b) wet O<sub>2</sub> and (c) dry O<sub>2</sub> annealing.

#### Acknowledgement

We are deeply indebted to I. K. Han and Y. H. Lee at KIST for helpful discussions during the course of this work. We would also like to thank S. R. Lee at ISRC and J. O. Lee at KSRI for the Si bonding process and the measurement of ultrasonic images, respectively.

#### References

1. L. CRISTEL, K. PETERSEN, P. BARTH, F. POURAHMADI, J. MALLON Jr and J. BRYZEK, *Sensors and Actuat.* A21–A23 (1990) 84.

2. K. PETERSEN, J. BROWN, T. VERMEULEN, P. BARTH, J. MALLON Jr and J. BRYZEK, *ibid* **A21–A23** (1990) 96.
3. M. SHIMBO, K. FURUKAWA, K. FUKUDA and K. TANZAWA, *J. Appl. Phys.* **60** (1986) 2987.
4. H. OHASHI, K. FURUKAWA, M. ATSUTA, A. NAKAGAWA and K. IMAMURA, *Proc. IEDM* **87** (1987) 678.
5. Q.-Y. TONG, X.-L. XU and H. SHEN, *Electron. Lett.* **26** (1990) 697.
6. J. B. LASKY, *Appl. Phys. Lett.* **48** (1986) 78.
7. W. P. MASZARA, *J. Electrochem. Soc.* **138** (1991) 341.
8. K. C. LEE, *ibid* **137** (1990) 2556.
9. W. KERN and D. A. PUOTINEN, *RCA Rev.* **31** (1970) 187.
10. W. P. MASZARA, G. GOETZ, A. CAVIGLIA and J. B. McKITTRICK, *J. Appl. Phys.* **64** (1988) 4943.
11. R. STENGL, T. TAN and U. GOSELE, *Jpn. J. Appl. Phys.* **28** (1989) 1735.
12. K. W. LEE and K. D. WISE, *IEEE Trans. Electron Dev.* **ED-29** (1982) 34.
13. C. M. OSBURN and D. W. ORMOND, *J. Electrochem. Soc.* **119** (1972) 591.
14. J. L. MOLL, *Proc. IRE* **46** (1958) 1076.

*Received 2 September 1991  
and accepted 30 July 1992*